Modelling dielectric losses in microstrip traveling-wave kinetic-inductance parametric amplifiers

D. Valenzuela, F.P. Mena, and J. Baselmans.

Abstract— **The development of travelling-wave kinetic inductance parametric amplifiers has introduced a promising new technology in radio astronomy [1]. In fact, it has the potential to reach near quantum-limited noise on a wider bandwidth, larger dynamic range and higher operation frequency when compared with current technologies. While the first implementation of a TKIPA used a coplanar waveguide for the transmission line [1], in this work, we present simulation studies using a microstrip line. One of the main motivations is to be able to obtain a 50-Ω line suitable for readily connection with other components. Therefore, reducing the reflections produced by an impedance mismatch between the ports. In this work we present the design of two different 50-Ω microstrip engineered transmission lines for parametric amplification using the four- and three-wave mixing effects. Additionally, we have included losses in the model. We have simulated their dispersion relation, and the parametric gain with pump frequencies at 7 and 14 GHz for the four- and three-wave mixing effects, respectively. We demonstrate that the three-wave mixing process requires less pumping power for obtaining the same gain with the added advantage of not having a stop band within the operation range. Furthermore, our simulations demonstrate that three-wave mixing is less affected by losses on the transmission line.**

Index Terms— **Filters, microwave, parametric, superconductors.**

I. INTRODUCTION

HIGH electron mobility transistors have been especially useful in astronomy. Amplifiers based on it are reliable, stable, and can work in an octave or higher bandwidth without increasing the noise significantly. However, their added noise reach between 10-20 times the quantum limit, depending on the operation frequency. Recently, a new kind of amplifiers, namely the traveling-wave kinetic inductance parametric amplifiers (TKIPA), have been the focus of attention due to its promising properties. The TKIPA makes use of the non-linear kinetic inductance of a superconductor, which is constructed as transmission line, to produce parametric amplification. In this process, amplification occurs when a weak signal, f_s, is fed into the line in the presence of a strong pump signal, f_p. Since the kinetic inductance depends quadratically with current, interaction of four photons in the form of four wave mixing (FWM) is expected. Conservation of energy requires that an additional idle signal, f_i, is created according to

$$f_s + f_i = 2f_p.$$

Unwanted harmonics of the pump and target signal are suppressed by constructing the transmission line as a periodic-structure filter, which results in a concentration of power in the desire bandwidth. While the first implementation of a TKIPA has used a coplanar waveguide for the transmission line [1], in
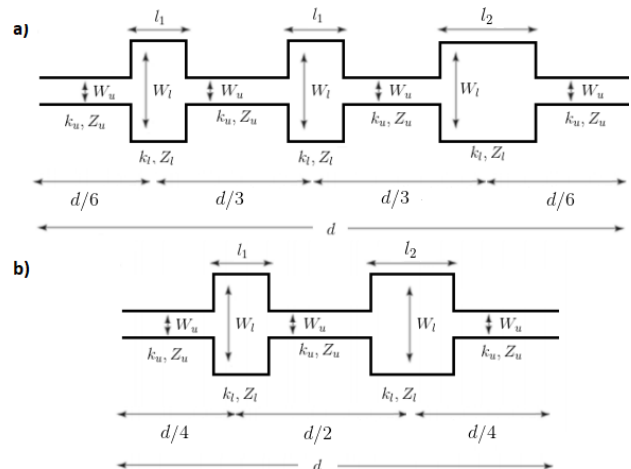

Fig. 1. Unit cells of the periodic filter used to implement the parametric amplifier. The geometrical parameters d, W_u, W_l, l_1, and l_2 were optimized as to select the desired operation frequency, and location and strength of the stop bands. The widths of the lines, W_u and W_l, define their propagation constants, k_u and k_l, and characteristic impedances, Z_u and Z_l. a) Cell supporting FWM. b) Cell supporting TWM.

D. Valenzuela is with the Electrical Engineering Department, Universidad de Chile, Santiago, Chile.

F. P. Mena is with Electrical Engineering Department and with the Millimeter Wave Lab, Universidad de Chile, Santiago, Chile (e-mail: fpmena@uchile.cl).

J. Baselmans is with the Electrical Engineering Department of Delft University of Technology and with the Netherlands Institute for Space Research, The Netherlands.
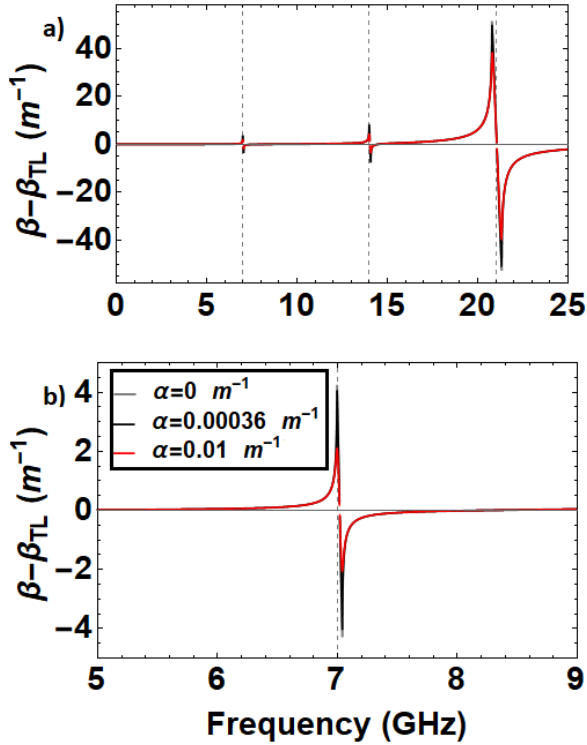
Fig. 2. Simulated dispersion relation of an engineered transmission line that uses FWM, with different losses. The difference $\Delta\beta = \beta - \beta_{TL}$ is illustrated to observe only the generated stopbands. a) The first stopband is located near the pump frequency f_p at 7 GHz. An important stop-band is produced at $3f_p$ to produce FWM. b) Zoom of the first stopband.

Fig. 3. Equivalent attenuation constant α_t of the periodic FWM transmission line. (a) Different values of losses α were added to the cell. It has been assumed that the unloaded and loaded elements have the same amount of losses. (b) Zoom to appreciate the effect of losses when $\alpha = 0.00036 \ \mathrm{m}^{-1}$.

this work, we present simulation studies using a microstrip line. One of the main motivations is to be able to obtain a 50-Ω line suitable for readily connection with other components. Preliminary studies have shown that the necessary geometry and dimensions is achievable when using common substrates as amorphous Si [3]. However, given the necessary thickness of the substrate, the line may be prone to high dielectric losses. Therefore, we have included them in our simulations. Furthermore, we have included a DC current, I_{DC}, feeding the system, as a method to reduce the amplitude of the pump current. When I_{DC} is included, a linear part appears in the kinetic inductance. If $I_{DC} > I_{RF}/2$, the linear part dominates over the quadratic part, and therefore, the parametric process of three-wave mixing (TWM) is produced [4]. In this case, conservation of energy also requires the creation of an idle signal according to

$$f_s + f_i = f_p.$$

In this work we compare the two parametric process, FWM and TWM.

II. DESIGN & SIMULATIONS

The design starts by selecting the appropriate microstrip configuration. We have selected NbTiN ($\rho_n = 150 \ \Omega.cm$, $T_c = 15.1$ K) deposited over amorphous Si ($\epsilon_r = 10$). Given the available deposition process, a thickness of 250 μm for the substrate was selected. Furthermore, thicknesses of 60 and 300 nm were selected for the strip and the ground, respectively.
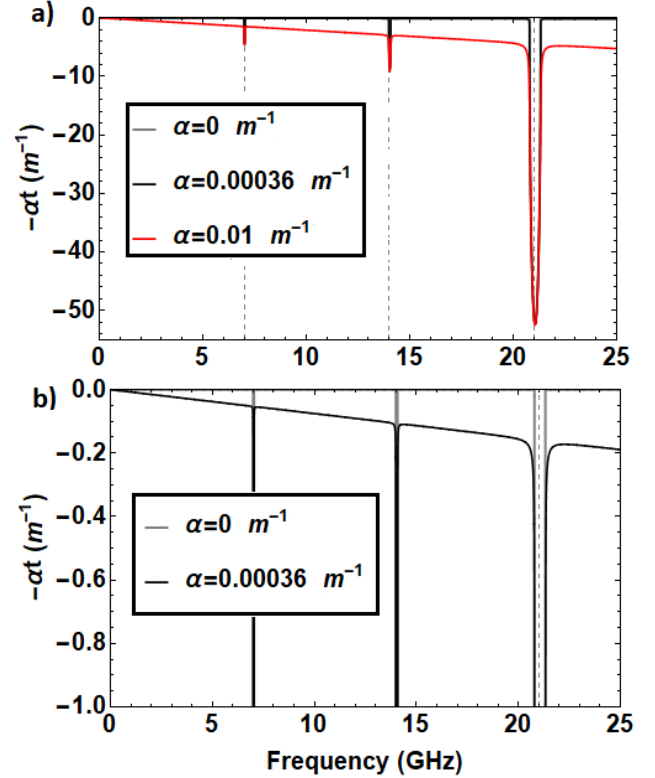
Preliminary measurements using microstrip resonators have demonstrated that microstrips with a loss of $\alpha = 0.00036 \ \mathrm{m}^{-1}$ (equivalent to $\tan \delta = 1.2 \times 10^{-6}$) can be fabricated [3]. To appreciate more clearly the effect of losses, we have also used an *ad-hoc* value of $\alpha = 0.01 \ \mathrm{m}^{-1}$ in the simulations described below. Furthermore, for the simulations we have used $J_c = 10^7 \ \mathrm{A.m}^{-2}$ [5].

An scheme of the FWM engineered transmission line is shown in Fig. 1a. It is divided in seven transmission lines. The first four are the *unloaded* elements, that is to say, the lines that are used as a coupling to the external ports. Each of them are interleaved with three perturbations or *loaded* elements. The scheme of the TWM filter is shown in figure 1b. In this case the cell is divided in five transmission lines. The main characteristic of both filters is their propagation constant, $\gamma = \alpha_t + j\beta$, which is calculated using the ABCD matrix of the cell and assuming that the transmission line supports the propagation of a traveling-wave. We have added an attenuation constant independent of frequency in the propagation constants k_u and k_l during the calculation of the ABCD matrices. The dimensions of the filter were tuned to create stopbands at harmonics of the pump frequency. The parametric effect was simulated using the couple mode equations [6].
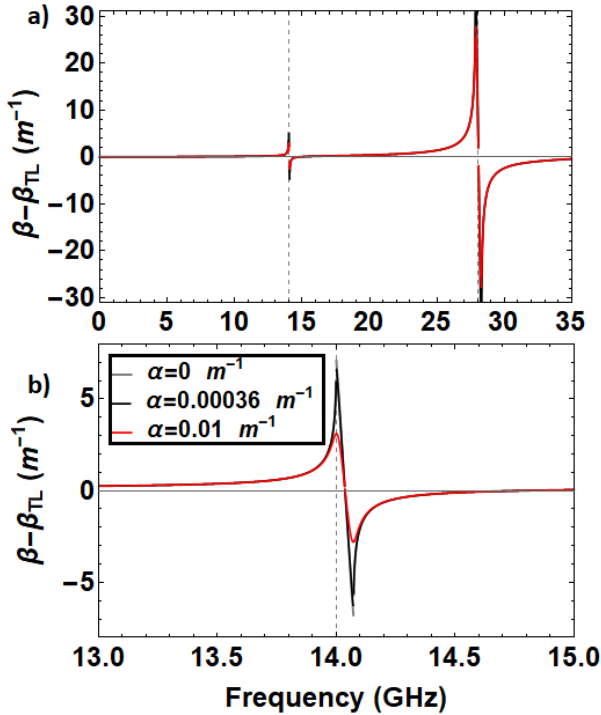
Fig. 4. Dispersion relation of the periodic transmission line, in TWM, expressed as $\Delta\beta = \beta - \beta_{TL}$. The first stopband is located at $2f_p$ to improve the amplification for TWM.

III. RESULTS

A. Four wave mixing

Fig. 2a illustrates the propagation constant β of the cell subtracted by the wave number of the unloaded segment β_{TL}, $\Delta\beta = \beta - \beta_{TL}$. It can be noted that the stopbands are located near or at harmonics of the pump frequency, $f_p = 7$ GHz. The first one, located near f_p, has a width of approximately 30 MHz. The additional dispersion around this stop band produces additional parametric amplification. The second stop-band, located near $2f_p$ with a bandwidth of 90 MHz, does not have an important impact on the amplifier. The third stop-band is located at $3f_p$ with a bandwidth of 920 MHz, which is considerably wider than the other two stop bands. This effect is expected, due to the need of removing frequencies above $3f_p$, so the power of the amplifier can be concentrated in desirable frequencies. A close up of $\Delta\beta$ around the first stop band is shown in Fig. 2b. It can be noted that an increment of the attenuation constant in the line generates a smoother curve. This behavior can be explained as a *deterioration* of the propagation constant. Losses decrease the dispersion in the transmission line, which could allow the propagation of undesirable signals. The equivalent attenuation constant α_t of the periodic filter is observed in Fig. 3. It can be seen that its value increases with the attenuation constant α for each of the sub-lines that compose the filter.

B. Three-wave mixing

The dispersion relation of the TWM transmission line can be observed in Fig. 4a. The pump frequency has been changed to
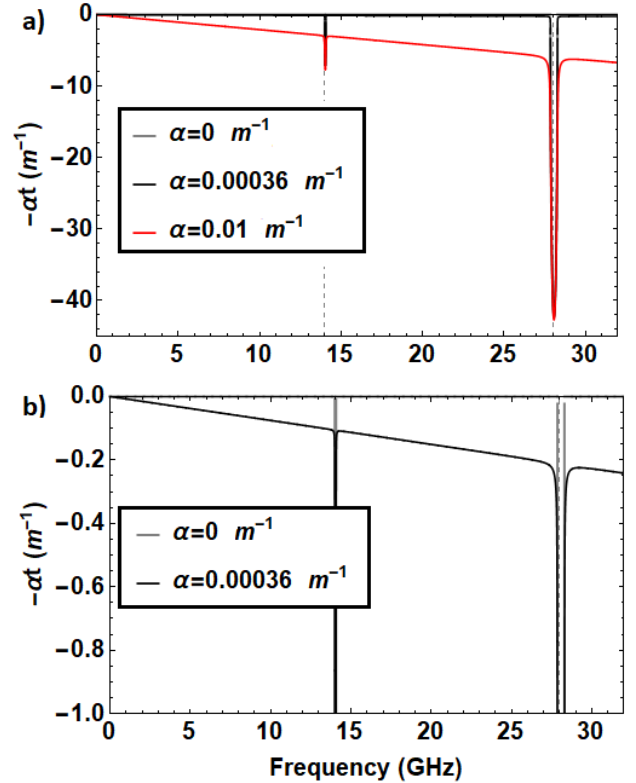

Fig. 5. Equivalent attenuation constant α_t of the periodic TWM transmission line. (a) Different values of losses α were added to the cell. It has been assumed that the unloaded and loaded elements have the same amount of losses. (b) Zoom to appreciate the effect of losses when $\alpha = 0.00036$ m^{-1}.

$f_p = 14$ GHz, so it can be compared with the parametric gain that uses the FWM effect. The first stop-band located near f_p has a bandwidth of approximately 100 MHz, but lays outside the operation range. It can be observed that the second stop-band at $2f_p = 28$ GHz has a bandwidth of ≈ 450 MHz, much wider when compared with the first stopband. In TWM, the deterioration of the propagation constant is also present, where a large attenuation constant generates a smoother stopband at the harmonics of the pump frequency. The equivalent attenuation constant α_t is shown in Fig. 5. It also presents a degradation of the stopbands when the attenuation constant of the original line increases. Furthermore, this decrement is larger at $2f_p$, where this harmonic is expected to be suppressed.

C. Parametric Gain

Fig. 6 presents the simulated parametric gain, including dielectric loses, of two 50-Ω microstrip lines. A DC bias equal to 13% of the effective critical current was used in TWM as to obtain a similar gain to that obtained in FWM. Two important results are highlighted. First, the inclusion of a DC bias results in a parametric gain that is not affected considerably when losses are included. Secondly, TWM allows obtaining similar gain than FWM with a lower amplitude of the pump signal.

IV. CONCLUSIONS & FUTURE WORK

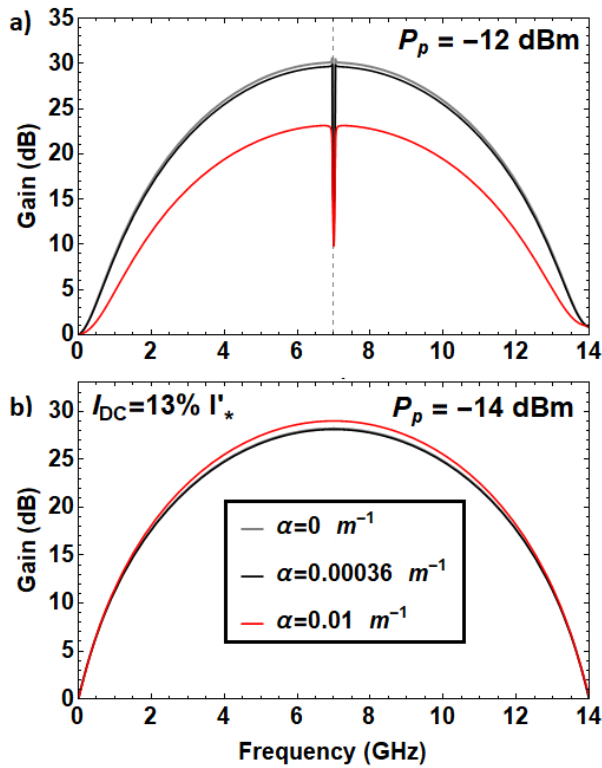In summary, we have designed and simulated two engineered transmission lines for use with three- and four-wave mixing.

Fig. 6. Simulated parametric gain of devices, including losses of the substrate. (a) FWM and (b) TWM. The parameter P_p corresponds to the power of the pump signal, and $I'_* = I_C/2\alpha$ is the effective critical current, where α is the fraction of kinetic inductance.

We have calculated their propagation constants and parametric gains. We observe that the design which uses three-wave mixing needs less pumping power to obtain the same gain as when four-wave mixing is used. Moreover, our simulations demonstrate that three-wave mixing is less prone to be affected by dielectric losses with the added advantage that the first stop band lays outside the operation range.

Since this work demonstrates that including losses degrades the stop bands of the engineered transmission lines, we are working on simulating the effect of having undesired tones travelling in the line. Furthermore, we are working on implementing the parametric amplifiers described here.

<div align="center">REFERENCES</div>

[1] B. Eom, P. Day, H. LeDuc and J. Zmuidzinas, "A wideband, low-noise superconducting amplifier with high dynamic range," *Nature,* vol. 623, 2012.

[2] S. Aanlange and H. Snortland, "A current controlled variable delay superconducting transmission line," *in IEEE Transactions on Magnetics,* pp. 1388-1391, 1989.

[3] F. Mena, «Internal report».

[4] M. Vissers, R. Erickson, H. Ku, L. Vale, X. Wu, G. Hilton and D. Pappas, "Low-noise kinetic inductance traveling-wave amplifier using three-wave mixing," *Applied physics letter,* vol. 108, 2016.

[5] A. Klimov, W. Sysz, M. Guziewicz, V. Kolkovsky, I. Zaytseva and A. Malinowski, "Characterization of the critical current and physical properties of superconducting epitaxial NbTiN sub-micron structures," *Physica C: Superconductivity and its Applications,* vol. 536, pp. 35-38, 2017.

[6] G. Agrawal, Nonlinear fiber optics, 2001.